Impulse noise mitigation for MIMO-OFDM wireless networks with linear equalization

Donatella Darsena

Dipartimento di Ingegneria
Università Parthenope di Napoli
Centro Direzionale Isola C4,
I-80143, Napoli, Italy,
Email: darsena@uniparthenope.it

Giacinto Gelli, Fulvio Melito, Francesco Verde, Andrea Vitiello

Dipartimento di Ingegneria Elettrica
e Tecnologie dell'Informazione
Università Federico II di Napoli
Via Claudio 21, I-80125, Napoli, Italy,
Email: [gelli, fulvio.melito, f.verde]@unina.it

***Abstract*—This paper considers a multiple-input multiple-output (MIMO) orthogonal frequency-division multiplexing (OFDM) wireless network contaminated by Middleton Class A impulsive noise, which is one of the major sources of performance degradation in many wireless systems, including sensor networks. In this scenario, the conventional linear zero-forcing (ZF) equalizer does not perform satisfactorily, since the diversity order does not monotonically increase with the signal-to-noise ratio (SNR). In order to overcome such a problem, we synthesize an improved linear ZF equalizer, which mitigates, in the minimum mean output-energy (MMOE) sense, the impulse noise contribution at the equalizer output. Specifically, the proposed equalizer exploits the fact that the noise samples can be spatially correlated in compact multi-antenna receivers, i.e., when the antenna elements cannot be sufficiently spaced apart due to size constraints. Numerical simulations are performed, aimed at comparing the performances of the proposed ZF-MMOE equalizer with those of competing approaches.**

I. Introduction

When dealing with transmission over frequency-selective channels, multiple-input multiple-output (MIMO) orthogonal frequency-division multiplexing (OFDM) wireless systems [1], [2] are emerging as the preferred solution to achieve high spectral efficiency, coupled with diversity and multiplexing gains. Design and analysis of MIMO-OFDM transceivers, aimed at exploiting spatial diversity, is often carried out assuming an additive white Gaussian noise (AWGN) model for the disturbance, with the additional presence of narrowband interference [3]. However, together with multipath fading, impulsive (non-Gaussian) noise, generated by natural (e.g., atmospheric noise) as well as artificial (e.g., ignition noise) sources, can be the dominant cause of performance degradation [4], [5] in many wireless applications, including sensor networks.

Performance analysis of co-located and distributed MIMO wireless networks in impulsive noise has been considered in [6], [7] and [8], [9], [10], respectively, by adopting the well known *Middleton Class A* (MCA) [11], [12], [13] model for the noise. In these works, the underlying channels are modeled as frequency-flat Rayleigh block-fading systems, and the MCA noise samples at the receiver are assumed to be either statistically independent, or statistically dependent but spatially uncorrelated. In many applications (e.g., sensor networks), the receiver is a simple and compact device, which makes antenna separations of several wavelengths impractical: thus, the MCA noise samples might become spatially correlated [14]. Moreover, the limited computational capability dictates the use of low-complexity equalization structures.

To jointly counteract the effects of frequency-selective fading and MCA additive noise, an effective solution is the adoption at the receiver of a simple linear equalizer. In the presence of impulse noise, however, the conventional zero-forcing (ZF) algorithm might perform poorly, since no specific measure is undertaken to counteract the noise effects. A common approach [15] to improve performance consists of inserting a memoryless nonlinearity (clipping, blanking, or a combination thereof) before the ZF equalizer. However, since signal blanking/clipping is a nonlinear operation, it distorts the signal constellation and, even worse, destroys orthogonality among OFDM subcarriers, thus resulting into intercarrier interference (ICI).

In this paper, we propose an alternative solution, which assures remarkable performance improvements compared to both the conventional ZF equalizer and the simple memoryless nonlinearity approach, while only slightly increasing the overall receiver complexity. Specifically, we design an improved linear ZF equalizer, which exploits the spatial correlation among the MCA noise samples to mitigate, in the minimum mean output-energy (MMOE) [16] sense, the effects of the MCA noise at the receiver output. Monte Carlo numerical simulations, carried out in different operative scenarios in terms of average symbol-error-probability (ASEP) and finite SNR diversity order, corroborate the effectiveness of the proposed ZF-MMOE equalizer in comparison with existing receivers.

A. Notations

The fields of complex and real numbers are denoted with $\mathbb{C}$ and $\mathbb{R}$, respectively; matrices [vectors] are denoted with upper [lower] case boldface letters (e.g., $\mathbf{A}$ or $\mathbf{a}$); the field of $m \times n$ complex [real] matrices is denoted as $\mathbb{C}^{m\times n}$ [$\mathbb{R}^{m\times n}$], with $\mathbb{C}^{m}$ [$\mathbb{R}^{m}$] used as a shorthand for $\mathbb{C}^{m\times 1}$ [$\mathbb{R}^{m\times 1}$]; the notations $(\cdot)^{\mathrm{T}}$, $(\cdot)^{\mathrm{H}}$, $(\cdot)^{-1}$, and $(\cdot)^{\dagger}$ denote the transpose, the conjugate transpose, the inverse, and the Moore-Penrose generalized inverse of a matrix, respectively; $\mathbf{0}_m \in \mathbb{R}^m$, $\mathbf{O}_{m\times n} \in \mathbb{R}^{m\times n}$ and $\mathbf{I}_m \in \mathbb{R}^{m\times m}$ denote the null vector, the null matrix, and the identity matrix, respectively; $\|\mathbf{A}\|^2 \triangleq \mathrm{tr}(\mathbf{A}\,\mathbf{A}^{\mathrm{H}}) = \mathrm{tr}(\mathbf{A}^{\mathrm{H}}\mathbf{A})$ is

the squared Frobenius norm of $\mathbf{A} \in \mathbb{C}^{m\times n}$, which boils down to the squared Euclidean norm of a vector when $n = 1$; a circular symmetric complex Gaussian random vector $\mathbf{x} \in \mathbf{C}^n$ with mean $\boldsymbol{\mu} \in \mathbb{C}^n$ and covariance matrix $\mathbf{K} \in \mathbb{C}^{n\times n}$ is denoted as $\mathbf{x} \sim \mathcal{CN}(\boldsymbol{\mu}, \mathbf{K})$.

B. Univariate MCA noise model

Under the MCA model [11], [12], [13], each noise sample is expressed as a zero-mean complex circular random variable (RV) $w = n + i$, where $n \in \mathcal{CN}(0, \sigma_n^2)$ is Gaussian thermal noise, whereas i models the non-Gaussian impulsive component, with variance σ_i^2. The probability density function (pdf) of w can be expressed as a weighted sum of conditionally-Gaussian univariate pdfs as follows:

$$p_w(v) = \sum_{k=0}^{+\infty} \alpha_k \, p_{w|k}(v|k) \,, \qquad v \in \mathbb{C} \tag{1}$$

where $\alpha_k \triangleq e^{-\lambda} \left(\lambda^k/k!\right)$, with $\lambda > 0$ the *impulsive index*, represents the probability that k noise pulses are affecting the receiver, and

$$p_{w|k}(v|k) = \frac{1}{\pi \, \sigma_k^2} \, \exp\left(-\frac{|v|^2}{\sigma_k^2}\right) . \tag{2}$$

For any $k \geq 0$, the parameter σ_k^2 in (2) represents the conditional variance of w, which can be expressed as $\sigma_k^2 = \sigma_w^2 \beta_k$, where $\sigma_w^2 = \sigma_n^2 + \sigma_i^2$ is the variance of w, and

$$\beta_k \triangleq \frac{k \, \lambda^{-1} + \Gamma}{1 + \Gamma} \tag{3}$$

with $\Gamma \triangleq \sigma_n^2/\sigma_i^2 > 0$ the *Gaussian ratio*.

The parameters λ and Γ control the shape of the pdf in the MCA model, i.e., the degree of impulsiveness of the noise: for $\lambda \ll 1$, the noise becomes more and more impulsive, whereas for $\lambda \geq 1$ the noise tends to be Gaussian. Similarly, for small values of Γ, the noise becomes more impulsive, while it tends to be Gaussian for large values of Γ.

II. System model and basic assumptions

The considered MIMO system is composed by a transmitter and a receiver equipped with N_T and N_R antennas, respectively. The transmitter employs a MIMO-OFDM modulation with spatial multiplexing over M subcarriers [1], [2]. The wireless channel between each pair of antennas is modeled as a linear time-invariant finite-impulse response system, whose order does not exceed the OFDM cyclic prefix (CP) length L_cp; additionally, all the channels are assumed to be *quasi static*, i.e., their impulse responses are fixed during the transmission of one OFDM symbol, but are allowed to change from one symbol to another. Perfect symbol synchronization between the transmitter and the receiver is assumed, and channel state information is known only at the receiver via training, but is unknown at the transmitter.

A. Transmitted signal

Let $\mathbf{s}^{(m)} \triangleq [s_1^{(m)}, s_2^{(m)}, \ldots, s_{N_\mathrm{T}}^{(m)}]^\mathrm{T} \in \mathbb{C}^{N_\mathrm{T}}$ collect the symbols to be transmitted by the transmitter on the mth OFDM subcarrier, with $m \in \{0, 1, \ldots, M-1\}$. Hereinafter, we assume that: **(a1)** $\mathbf{s}^{(m)}$ is a zero-mean circularly symmetric complex random vector with autocorrelation matrix $\mathbb{E}[\mathbf{s}^{(m)} \, \mathbf{s}^{(m)\mathrm{H}}] = \mathbf{I}_{N_\mathrm{T}}$, and whose entries assume independent and identically distributed (i.i.d.) equiprobable values in the constellation set $\mathcal{S}$ of cardinality Q. The symbol block $\mathbf{s}^{(m)}$ is processed by a scaled unitary channel-independent precoder, obtaining thus $\tilde{\mathbf{s}}^{(m)} \triangleq \mathbf{F}_0^{(m)} \, \mathbf{s}^{(m)} \in \mathbb{C}^{N_\mathrm{T}}$, with $\mathbf{F}_0^{(m)\mathrm{H}} \, \mathbf{F}_0^{(m)} = \mathbf{F}_0^{(m)} \, \mathbf{F}_0^{(m)\mathrm{H}} = {N_\mathrm{T}}^{-1} \, \mathbf{I}_{N_\mathrm{T}}$, which ensures that $\mathbb{E}[\|\tilde{\mathbf{s}}^{(m)}\|^2] = 1$. Before being transmitted, the elements of the precoded data-blocks $\tilde{\mathbf{s}}^{(m)}$, for $m \in \{0, 1, \ldots, M-1\}$, corresponding to the same antenna index are subject to OFDM processing, encompassing M-point inverse discrete Fourier transform (IDFT) followed by CP insertion.

B. Received signal and multivariate MCA noise model

After discarding the CP and performing M-point discrete Fourier transform (DFT), the received signal at the mth subcarrier is given by

$$\mathbf{r}^{(m)} = \mathbf{H}^{(m)} \, \tilde{\mathbf{s}}^{(m)} + \mathbf{w}^{(m)} = \mathbf{C}^{(m)} \, \mathbf{s}^{(m)} + \mathbf{w}^{(m)} \tag{4}$$

for $m \in \{0, 1, \ldots, M-1\}$, where the matrix $\mathbf{H}^{(m)} \in \mathbb{C}^{N_\mathrm{R}\times N_\mathrm{T}}$ collects the mth DFT samples of the MIMO channel, $\mathbf{C}^{(m)} \triangleq \mathbf{H}^{(m)} \, \mathbf{F}_0^{(m)} \in \mathbb{C}^{N_\mathrm{R}\times N_\mathrm{T}}$ is the *combined* channel-precoder matrix, and $\mathbf{w}^{(m)} \triangleq [w_1^{(m)}, w_2^{(m)}, \ldots, w_{N_\mathrm{R}}^{(m)}]^\mathrm{T} \in \mathbb{C}^{N_\mathrm{R}}$ accounts for noise at the mth DFT bin.

We assume that: **(a2)** the entries of $\mathbf{H}^{(m)}$, which is statistically independent of $\mathbf{s}^{(m)}$ and $\mathbf{H}^{(p)}$, for $m \neq p$, are i.i.d. $\mathcal{CN}(0, \sigma_h^2)$ RVs, whose variance depends on the average path loss associated to the link between the transmitter and the receiver; **(a3)** the random matrix $\mathbf{H}^{(m)}$ is full-column rank, i.e., $N_\mathrm{R} \geq N_\mathrm{T}$ and $\mathrm{rank}[\mathbf{H}^{(m)}] = N_\mathrm{T}$, with probability 1; **(a4)** the vector $\mathbf{w}^{(m)}$ is statistically independent of $\mathbf{s}^{(m)}$ and $\mathbf{H}^{(m)}$, with $\mathbf{w}^{(m)}$ statistically independent of $\mathbf{w}^{(p)}$, for $m \neq p$, whose pdf is a weighted sum of conditionally-Gaussian multivariate pdfs (see [14])

$$p_{\mathbf{w}^{(m)}}(\mathbf{v}) = \sum_{k=0}^{+\infty} \alpha_k \, p_{\mathbf{w}^{(m)}|k}(\mathbf{v}|k) \,, \qquad \mathbf{v} \in \mathbb{C}^{N_\mathrm{R}} \tag{5}$$

with

$$p_{\mathbf{w}^{(m)}|k}(\mathbf{v}|k) = \frac{1}{(\pi \, \beta_k)^{N_\mathrm{R}} \det(\mathbf{K_{ww}})} \, \exp\left(-\frac{\mathbf{v}^\mathrm{H} \mathbf{K_{ww}}^{-1} \mathbf{v}}{\beta_k}\right) \tag{6}$$

where α_k and β_k have been defined in Subsection I-B, whereas $\mathbf{K_{ww}} \triangleq \mathbb{E}[\mathbf{w}^{(m)} \, \mathbf{w}^{(m)\mathrm{H}}] \in \mathbb{C}^{N_\mathrm{R}\times N_\mathrm{R}}$ is a positive definite correlation matrix, with $\{\mathbf{K_{ww}}\}_{\ell\ell} = \sigma_w^2$ for $\ell \in \{1, 2, \ldots, N_\mathrm{R}\}$, which models the spatial correlation of the noise at the receiver.

Some comments regarding assumption **(a4)** are in order. It is noteworthy that the elements of $\mathbf{w}^{(m)}$ are zero-mean MCA RVs, whose marginal pdf is given by (1), with parameters Γ, λ, and variance $\sigma_w^2 \triangleq \mathbb{E}[|w_\ell^{(m)}|^2]$, for $\ell \in \{1, 2, \ldots, N_\mathrm{R}\}$. Moreover, the conditional variance of each element of $\mathbf{w}^{(m)}$ depends on the number k of noise pulses, while the correlation coefficient between any two entries of $\mathbf{w}^{(m)}$ is independent of k. Such a noise model can represent correlated or uncorrelated RVs: in particular, if $\mathbf{K_{ww}} = \sigma_w^2 \, \mathbf{I}_{N_\mathrm{R}}$, the RVs gathered in $\mathbf{w}^{(m)}$ are uncorrelated.[1] It is worth noting that eq. (5) cannot

[1] This corresponds to Model I considered in [6].

represent independent RVs, since (5) will not factor into the product of marginal pdfs.

III. Linear equalization structures

Since equalization at the receiver is carried out on a per-subcarrier basis, we will omit in the sequel the subcarrier index m. In order to recover $\mathbf{s}$, the received vector $\mathbf{r}$ in (4) is subject to *linear* equalization by means of a matrix $\mathbf{D} \triangleq [\mathbf{d}_1, \mathbf{d}_2, \ldots, \mathbf{d}_{N_\mathrm{T}}]^\mathrm{H} \in \mathbb{C}^{N_\mathrm{T} \times N_\mathrm{R}}$, with $\mathbf{d}_\ell \in \mathbb{C}^{N_\mathrm{R}}$ for $\ell \in \{1, 2, \ldots, N_\mathrm{T}\}$, thus yielding an estimate $\hat{\mathbf{s}} \triangleq [\hat{s}_1, \hat{s}_2, \ldots, \hat{s}_{N_\mathrm{T}}]^\mathrm{T} = \mathbf{D}\,\mathbf{r}$ of the symbol block $\mathbf{s}$, whose entries are finally quantized to the nearest symbols of $\mathcal{S}$.

A common choice for $\mathbf{D}$ in MIMO-OFDM systems is the ZF equalizer

$$\mathbf{D}_\mathrm{zf} = \mathbf{C}^\dagger \tag{7}$$

whose existence is assured by **(a3)**. The ZF equalizer turns out to be the minimum-norm (in the Frobenius sense) solution of the matrix equation $\mathbf{D}\,\mathbf{C} = \mathbf{I}_{N_\mathrm{T}}$.

Since the linear ZF equalizer cannot operate satisfactorily in impulse noise environments, we consider hereinafter an improved equalization strategy, based on the MMOE criterion [16] (also referred to [19] as the minimum variance distortionless response or Capon criterion), which offers a good compromise between performance and complexity.

A. ZF-MMOE equalizer

Under the assumption that $N_\mathrm{R} > N_\mathrm{T}$, the synthesis of the proposed ZF-MMOE equalizer is carried out by minimizing the conditional mean-output-energy $\mathrm{MOE}_\ell \triangleq \mathbb{E}[|\hat{s}_\ell|^2 \,|\, \mathbf{H}]$ for the ℓth symbol stream, subject to the *ZF constraint*, namely

$$\mathbf{D}_\text{zf-mmoe} = \arg\min_{\mathbf{D}} \mathbb{E}[\|\hat{\mathbf{s}}\|^2 \,|\, \mathbf{H}] \quad \text{s.t. } \mathbf{D}\,\mathbf{C} = \mathbf{I}_{N_\mathrm{T}} \tag{8}$$

whose solution is (see, e.g., [20], [21], [22])

$$\mathbf{D}_\text{zf-mmoe} = \left(\mathbf{C}^\mathrm{H}\,\mathbf{K}_\mathbf{rr}^{-1}\,\mathbf{C}\right)^{-1}\mathbf{C}^\mathrm{H}\,\mathbf{K}_\mathbf{rr}^{-1} \tag{9}$$

where $\mathbf{K}_\mathbf{rr} \triangleq \mathbb{E}[\mathbf{r}\,\mathbf{r}^\mathrm{H}] = \mathbf{C}\,\mathbf{C}^\mathrm{H} + \mathbf{K}_\mathbf{ww} \in \mathbb{C}^{N_\mathrm{R} \times N_\mathrm{R}}$ is the correlation matrix of $\mathbf{r}$, which can be directly estimated from the received data; in this case, finite-sample effects can be evaluated along the same lines of [17], [18]. It is apparent that the optimization problem (8) imposes N_T^2 linear constraints, which not only preserve the desired symbols, but also assure *deterministic* symbol separation.

The constrained optimization problem (8) can be reformulated as an unconstrained one, by resorting to an extension of the generalized sidelobe canceller decomposition [19], which was proposed in the array processing context. Specifically, it can be shown that $\mathbf{D}_\text{zf-mmoe}$ admits the canonical decomposition

$$\mathbf{D}_\text{zf-mmoe} = \underbrace{\mathbf{C}^\dagger}_{\mathbf{D}^{(\mathrm{f})}_\text{zf-mmoe}} - \underbrace{\boldsymbol{\mathcal{Y}}_\text{zf-mmoe}\,\boldsymbol{\Pi}}_{\mathbf{D}^{(\mathrm{a})}_\text{zf-mmoe}} = \mathbf{D}^{(\mathrm{f})}_\text{zf-mmoe} - \mathbf{D}^{(\mathrm{a})}_\text{zf-mmoe} \tag{10}$$

with

$$\begin{aligned}\boldsymbol{\mathcal{Y}}_\text{zf-mmoe} &\triangleq \mathbf{D}^{(\mathrm{f})}_\text{zf-mmoe}\,\mathbf{K}_\mathbf{rr}\,\boldsymbol{\Pi}^\mathrm{H}\left(\boldsymbol{\Pi}\,\mathbf{K}_\mathbf{rr}\,\boldsymbol{\Pi}^\mathrm{H}\right)^{-1} \\ &= \mathbf{D}^{(\mathrm{f})}_\text{zf-mmoe}\,\mathbf{K}_\mathbf{ww}\,\boldsymbol{\Pi}^\mathrm{H}\left(\boldsymbol{\Pi}\,\mathbf{K}_\mathbf{ww}\,\boldsymbol{\Pi}^\mathrm{H}\right)^{-1}\end{aligned} \tag{11}$$

where $\mathbf{D}^{(\mathrm{f})}_\text{zf-mmoe} = \mathbf{D}_\mathrm{zf} \in \mathbb{C}^{N_\mathrm{T} \times N_\mathrm{R}}$ represents the minimum-norm (in the Frobenius sense) solution of the ZF constraint imposed in (8), whereas the *signal blocking matrix* $\boldsymbol{\Pi} \in \mathbb{C}^{(N_\mathrm{R}-N_\mathrm{T}) \times N_\mathrm{R}}$ satisfies the relation $\boldsymbol{\Pi}\,\mathbf{C} = \mathbf{O}_{(N_\mathrm{R}-N_\mathrm{T}) \times N_\mathrm{T}}$, which leads to the second equality in (11). The choice of $\boldsymbol{\Pi}$ is not unique and, in the sequel, without loss of generality, we will only impose that $\boldsymbol{\Pi}\,\boldsymbol{\Pi}^\mathrm{H} = \mathbf{I}_{N_\mathrm{R}-N_\mathrm{T}}$.

Decomposition (10) enlightens the fact that $\mathbf{D}_\text{zf-mmoe}$ is the difference of a *fixed* (i.e., data-independent) term $\mathbf{D}^{(\mathrm{f})}_\text{zf-mmoe}$ and a *free* or *adaptive* term $\mathbf{D}^{(\mathrm{a})}_\text{zf-mmoe}$. Hence, with respect to the ZF equalizer, the additional implementation complexity of the ZF-MMOE solution consists of synthesizing $\mathbf{D}^{(\mathrm{a})}_\text{zf-mmoe}$, whose computational burden is mainly dictated by the matrix inversion $\left(\boldsymbol{\Pi}\,\mathbf{K}_\mathbf{ww}\,\boldsymbol{\Pi}^\mathrm{H}\right)^{-1}$, which approximatively requires $\mathcal{O}[(N_\mathrm{R} - N_\mathrm{T})^3]$ floating point operations. Moreover, it is important to observe that, in the absence of spatial correlation of the MCA noise at the receiver, i.e., when $\mathbf{K}_\mathbf{ww} = \sigma_w^2\,\mathbf{I}_{N_\mathrm{R}}$, the adaptive part of the CMMOE equalizer vanishes and $\mathbf{D}_\text{zf-mmoe} = \mathbf{D}_\mathrm{zf}$, i.e., it reduces to the ZF one (7).

IV. Numerical results

To assess the performance of the proposed approach, we present in this section the results of Monte Carlo computer simulations, where the performance of the ZF-MMOE equalizer (9) are compared with those of the conventional ZF equalizer and of the memoryless blanking approach [15] with optimized nonlinearity threshold (referred to as "ZF-blank"); as a reference, we also report the performance of the conventional ZF equalizer (referred to as "ZF-Gauss") in a classical Rayleigh-fading channel affected by additive colored Gaussian noise with correlation matrix $\mathbf{K}_\mathbf{ww}$.

The considered MIMO-OFDM system employs $M = 32$ subcarriers, with Gray-labeled QPSK ($Q = 4$) or 16-QAM ($Q = 16$) modulation on each subcarrier. As for the number of antennas, we simulate a MIMO $(N_\mathrm{T}, N_\mathrm{R}) = (2, 3)$ system configuration, where all the channels are generated according to assumptions **(a2)** and **(a3)**, with $\sigma_h^2 = 1$.

Regarding the noise correlation matrix $\mathbf{K}_\mathbf{ww}$, we adopt the following model:

$$\mathbf{K}_\mathbf{ww} = \sigma_w^2 \begin{bmatrix} 1 & \rho & \rho^2 \\ \rho^* & 1 & \rho \\ (\rho^2)^* & \rho^* & 1 \end{bmatrix} \tag{12}$$

where $\rho = |\rho|\,e^{j\measuredangle\rho}$ represents the correlation coefficient of the MCA noise between two adjacent antennas, with $|\rho|$ fixed either at 0.5 (low spatial correlation) or 0.9 (high spatial correlation), respectively, and $\measuredangle\rho$ is uniformly distributed in the interval $[0, 2\pi)$.

As performance measures, we adopt the average (over all spatial streams and subcarriers) symbol error probability (ASEP), defined as

$$\mathrm{ASEP} \triangleq \frac{1}{N_\mathrm{T}\,M\,\log_2(Q)} \sum_{\ell=1}^{N_\mathrm{T}} \sum_{m=1}^{M} \mathrm{P}_\ell^{(m)}(e) \tag{13}$$

where $\mathrm{P}_\ell^{(m)}(e)$ is the symbol error probability (SEP) in detecting the ℓth symbol stream $s_\ell^{(m)}$ on the mth subcarrier, and the

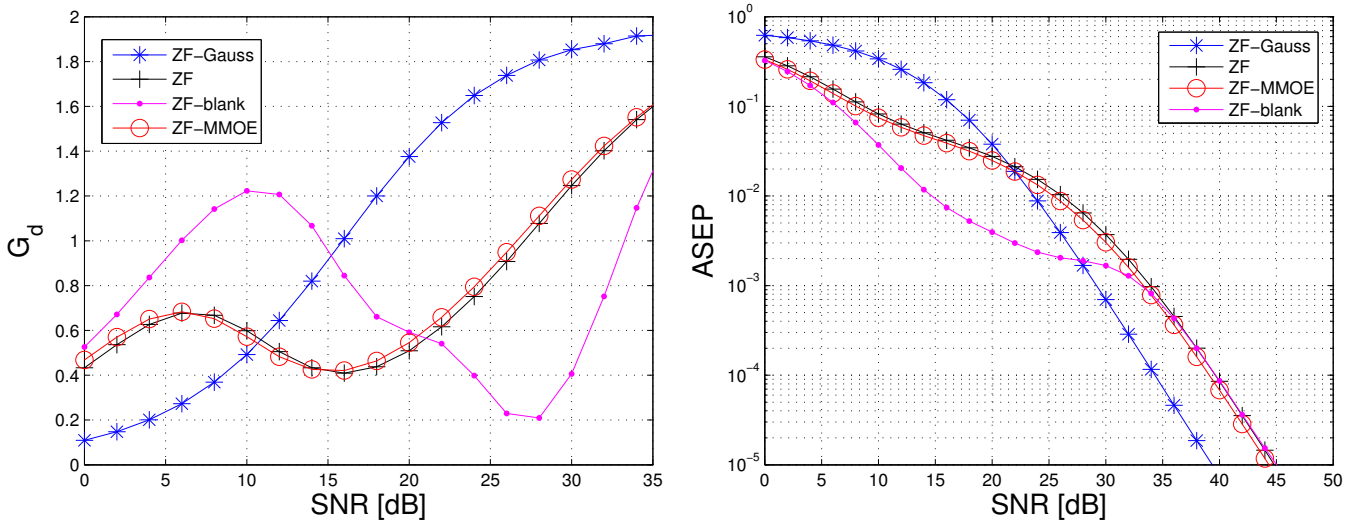

Fig. 1. Finite-SNR diversity order G_d and ASEP versus SNR for the receivers under comparison (QPSK modulation, $|\rho| = 0.5$).

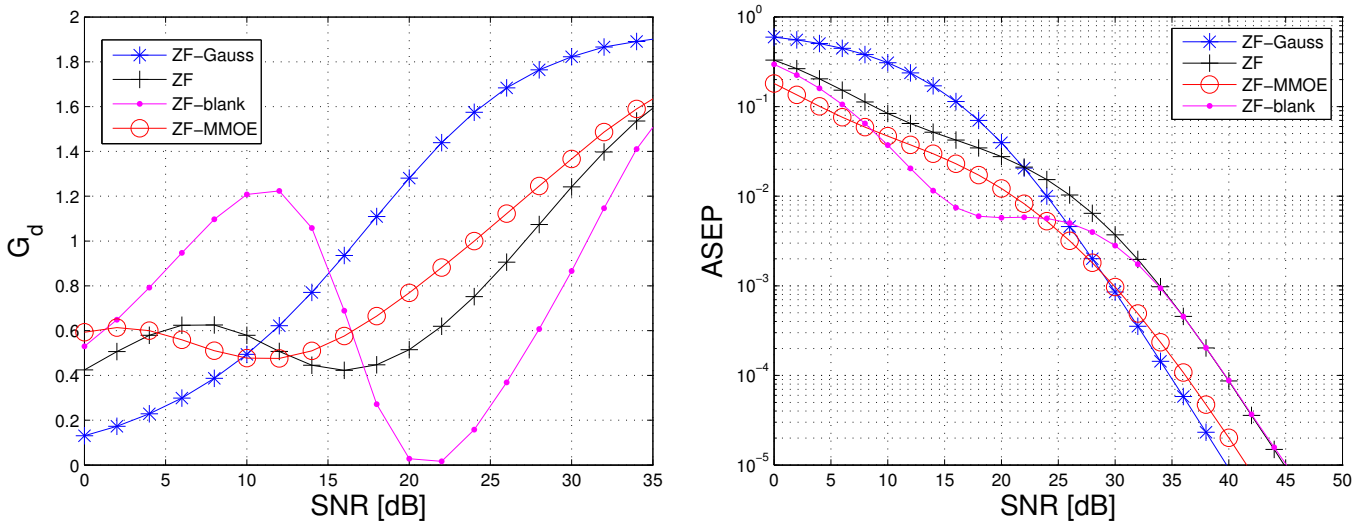

Fig. 2. Finite-SNR diversity order G_d and ASEP versus SNR for the receivers under comparison (QPSK modulation, $|\rho| = 0.9$).

finite-SNR diversity order G_d, which is defined as the negative slope of the log-log plot of the ASEP probability versus the SNR $\triangleq 1/\sigma_w^2$, i.e.,

$$\mathrm{G}_d \triangleq -\frac{\mathrm{d}\,\log(\mathrm{ASEP})}{\mathrm{d}\log(\mathrm{SNR})} = -\frac{\mathrm{SNR}}{\mathrm{ASEP}}\,\frac{\mathrm{d}(\mathrm{ASEP})}{\mathrm{d}(\mathrm{SNR})}\,. \qquad (14)$$

In each scenario, we carry out 10^5 independent Monte Carlo runs, with each run employing a different set of information symbols, noise samples, and fading channels.

Figs. 1 and 2 report both the finite-SNR diversity order G_d and the ASEP of the considered receivers as a function of the SNR in the case of QPSK modulation and for $|\rho| = 0.5$ and $|\rho| = 0.9$, respectively. It is apparent that, when the degree of spatial correlation is low (i.e., $|\rho| = 0.5$, see Fig. 1), the "ZF-blank" receiver provides the best performances, especially in the range 10–30 dB of SNR values, whereas all the receivers perform comparably for values of SNR exceeding 35 dB, showing a gap of about 5 dB with respect to the "ZF-Gauss" reference.

On the contrary, when the degree of spatial correlation is high (i.e., $|\rho| = 0.9$, see Fig. 2), the proposed ZF-MMOE equalizer outperforms both the conventional ZF and ZF-blank receivers in the moderate-to-high SNR region, ensuring an ASEP performance that is better or comparable to that of the "ZF-Gauss" reference. It can be observed that the "ZF-blank" is still superior, even in this high spatial correlation scenario, when the SNR values are in the range 10–25 dB.

It is worthwhile to observe that, in comparison with the "ZF-Gauss" reference, for all the receivers under comparison the diversity order exhibits a fluctuating behavior with the SNR, which is more pronounced for the "ZF-blank" one; nevertheless, for large values of SNR, the values of G_d for all receivers approach the asymptotical value of $N_\mathrm{R} - N_\mathrm{T} + 1 = 2$ typical of ZF equalization strategies [23].

Figs. 3 and 4 report again the diversity order G_d and ASEP

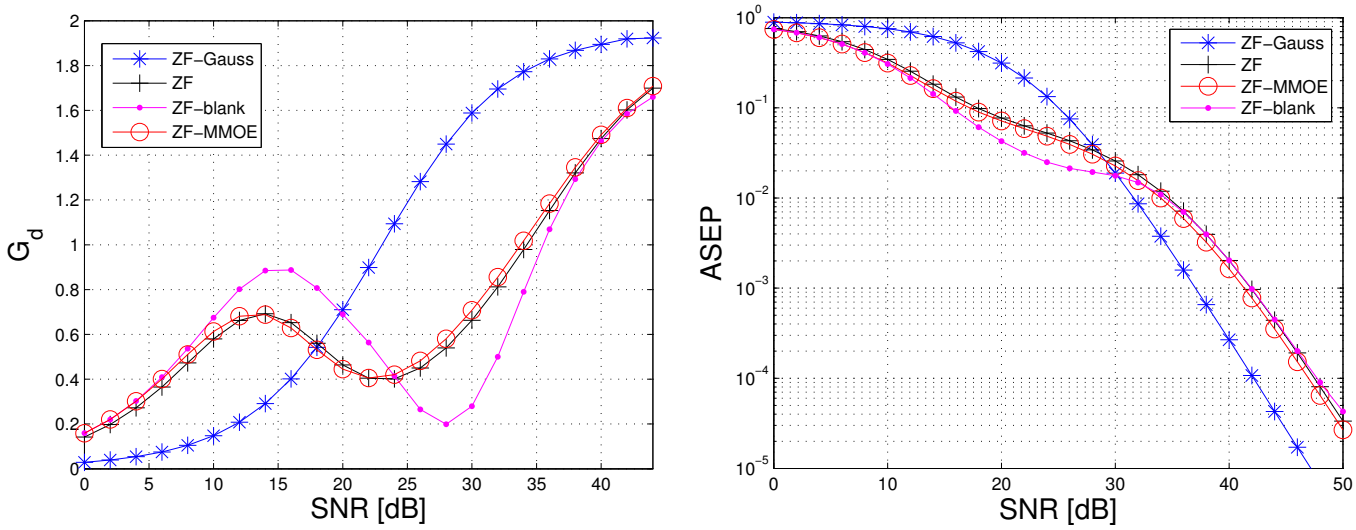

Fig. 3. Finite-SNR diversity order G_d and ASEP versus SNR for the receivers under comparison (16-QAM modulation, $|\rho| = 0.5$).

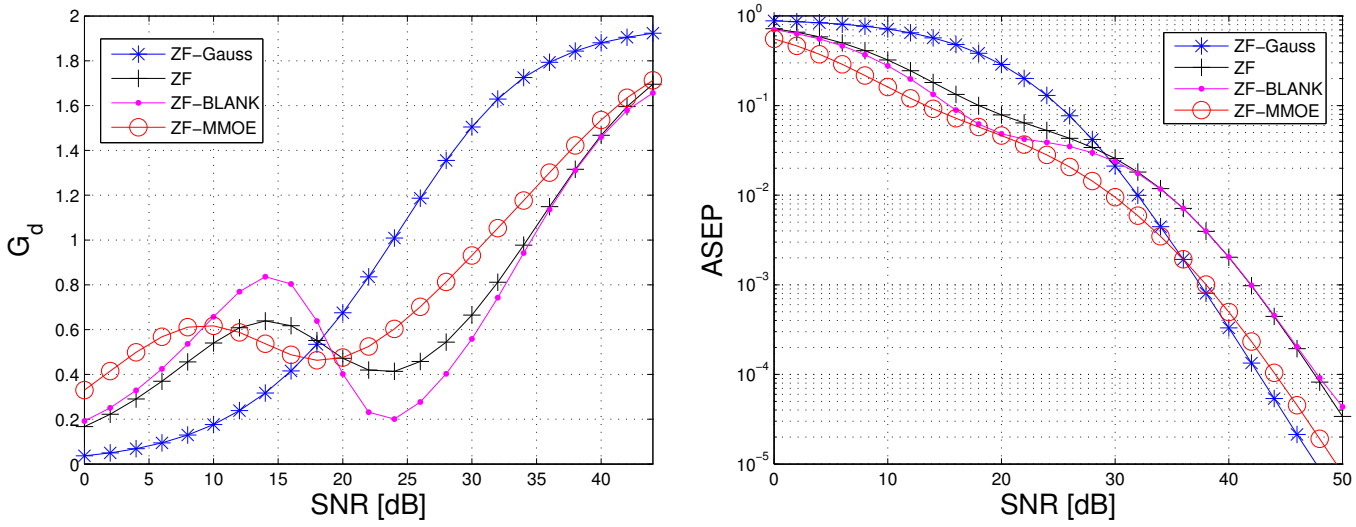

Fig. 4. Finite-SNR diversity order G_d and ASEP versus SNR for the receivers under comparison (16-QAM modulation, $|\rho| = 0.9$).

as a function of the SNR in the case of 16-QAM modulation and for $|\rho| = 0.5$ and $|\rho| = 0.9$, respectively. When the degree of spatial correlation is low (Fig. 3), the "ZF-blank" receiver is still able to outperform the other receivers, even though its performance advantage in the range 10–30 dB of SNR values is reduced, mainly due to the increased distortion and ICI of the 16-QAM constellation compared with the simpler QPSK one. When however the degree of spatial correlation is high (Fig. 4), the proposed ZF-MMOE equalizer provides the best performances over the whole region of SNR values, ensuring ASEP performances that are better than or comparable to those of the "ZF-Gauss" reference.

V. Conclusions

In this paper, we synthesized an improved ZF equalizer for a MIMO-OFDM system operating in the presence of impulse noise, described by the Middleton Class A model. Instead of employing the classical approach based of insertion of a memoryless non-linearity before OFDM demodulation, we designed a purely linear receiver based on the MMOE optimization criterion with a ZF constraint, which deterministically preserves the desired symbols without introducing neither constellation distortion nor ICI.

Simulation results have shown that the proposed ZF-MMOE receiver outperforms existing approaches in the presence of high spatial correlation between noise samples. Moreover, the performance advantage is more pronounced for higher-cardinality constellations, such as 16-QAM, which are widely employed in broadband communication systems. For simpler constellation like QPSK and low values of spatial noise correlation, the adoption of nonlinearity-based approaches (e.g., blanking) might be preferable, due to their low computational complexity.

REFERENCES

[1] D. Tse and P. Viswanath, *Fundamentals of Wireless Communication*, Cambridge University Press, 2005.

[2] Z. Wang and G. B. Giannakis, "Wireless multicarrier communications – Where Fourier meets Shannon," *IEEE Signal Processing Magazine*, vol. 17, no. 3, pp. 29–48, May 2000.

[3] D. Darsena, G. Gelli, L. Paura, and F. Verde, "NBI-resistant zero-forcing equalizers for OFDM systems," *IEEE Commun. Lett.*, vol. 9, no. 8, pp. 744–746, Aug. 2005.

[4] L. Angrisani, A. Napolitano, and M. Vadursi, "Modeling and measuring link capacity in communication networks," *IEEE Trans. Instrum. Meas.*, vol. 59, pp. 1065–1072, May 2010.

[5] A. Bondavalli, A. Ceccarelli, F. Gogaj, A. Seminatore, and M. Vadursi, "Experimental assessment of low-cost GPS-based localization in railway worksite-like scenarios," Measurement, vol. 46, pp. 456–466, Jan. 2013.

[6] C. Tepedelenlioglu and P. Gao, "On the diversity reception over fading channels with impulse noise," *IEEE Trans. Veh. Technol.*, vol. 54, pp. 2037-2047, Nov. 2005.

[7] P. Gao and C. Tepedelenlioglu, "Space-time coding over fading channels with impulsive noise" *IEEE Trans. Wireless Commun.*, vol. 6, pp. 220–229, Jan. 2007.

[8] S. Al-Dharrab and M. Uysal, "Cooperative diversity in the presence of impulse noise," *IEEE Trans. Wireless Commun.*, vol. 8, pp. 4730-4739, Sep. 2009.

[9] R. Savoia and F. Verde, "Performance analysis of decode-and-forward relaying in impulsive noise environments", *Proc. of Eighth Int. Symp. Wireless Commun. Systems (ISWCS)*, Aachen, Germany, Nov. 2011, pp. 412–416.

[10] R. Savoia and F. Verde, "Performance analysis of distributed space-time block coding schemes in Middleton Class A noise," *IEEE Trans. Veh. Technol.*, vol. 62, July 2013.

[11] D. Middleton, "Statistical-physical models of electromagnetic interference," *IEEE Trans. Electromagn. Compat.*, vol. 19, pp. 106–127, Aug. 1977.

[12] A.D. Spaulding and D. Middleton, "Optimum reception in the impulse interference environment – part I: coherent detection," *IEEE Trans. Commun.*, vol. 25, pp. 910–923, Sep. 1977.

[13] D. Middleton, "Procedure for determining the parameters of a first-order canonical models of class A and class B electromagnetic interference," *IEEE Trans. Electromagn. Compat.*, vol. 21, pp. 190–208, Aug. 1979.

[14] P.A. Delaney, "Signal detection in multivariate class-A interference," *IEEE Trans. Commun.*, vol. 43, pp. 365–373, Feb. 2006.

[15] S.V. Zhidkov, "Analysis and comparison of several simple impulse noise mitigation schemes for OFDM receivers," *IEEE Trans. Commun.*, vol. 56, pp. 5–9, Jan. 2008.

[16] M. Honig, U. Madhow, and S. Verdú, "Blind adaptive multiuser detection," *IEEE Trans. Inf. Theory*, vol. 41, pp. 944–960, July 1995.

[17] A.S. Cacciapuoti, G. Gelli, L. Paura, and F. Verde, "Finite-sample performance analysis of widely linear multiuser receivers for DS-CDMA systems," *IEEE Trans. Signal Process.*, vol. 56, no. 4, pp. 1572-1588, Apr. 2008.

[18] A.S. Cacciapuoti, G. Gelli, L. Paura, and F. Verde, "Widely-linear versus linear blind multiuser detection with subspace-based channel estimation: finite sample-size effects," *IEEE Trans. Signal Process.*, vol. 57, no. 4, pp. 1426-1443, Apr. 2009.

[19] H.L. Van Trees, *Optmimum Array Processing*. New York: John Wiley & Sons, 2002.

[20] G. Gelli and F. Verde, "Two-stage interference-resistant adaptive periodically time-varying CMA blind equalization," *IEEE Trans. Signal Process.*, vol. 50, pp. 662–672, Mar. 2002.

[21] D. Darsena, G. Gelli, L. Paura, F. Verde, "Widely-linear equalization and blind channel identification for interference-contaminated multicarrier systems", *IEEE Trans. Signal Process.*, vol. 53, pp. 1163-1177, March 2005.

[22] D. Darsena, G. Gelli, L. Paura, F. Verde, "A constrained maximum-SINR NBI-resistant receiver for OFDM systems," *IEEE Trans. Signal Process.*, vol. 55, pp. 3032-3047, June 2007.

[23] F. Verde, D. Darsena, and A. Scaglione, "Cooperative randomized MIMO-OFDM downlink for multicell networks: design and analysis," *IEEE Trans. Signal Process.*, vol. 58, pp. 384-402, Jan. 2010.